ChemComm

Accepted Manuscript

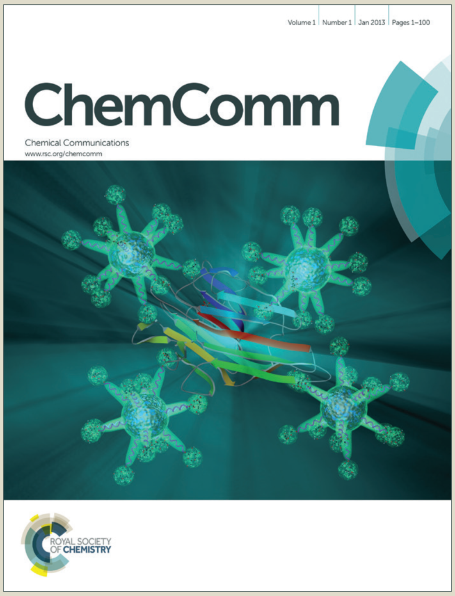

ROYAL SOCIETY OF CHEMISTRY

www.rsc.org/chemcomm

Chem Comm

ChemComm

Dynamic Article Links ►

Cite this: DOI: 10.1039/c0xx00000x

www.rsc.org/xxxxxx

ARTICLE TYPE

Low temperature *in situ* Raman spectroscopy of electro-generated arylbis(arylthio)sulfonium ion

Kouichi Matsumoto,[a]* Yu Miyamoto,[a] Kazuaki Shimada,[a] Yusuke Morisawa,[a] Hendrik Zipse,[b] Seiji Suga,[c] Jun-ichi Yoshida,[d] Shigenori Kashimura,[a] and Tomonari Wakabayashi[a]*

Received (in XXX, XXX) Xth XXXXXXXXX 20XX, Accepted Xth XXXXXXXXX 20XX
DOI: 10.1039/b000000x

A low temperature *in situ* Raman spectroscopic method was developed for the detection of unstable intermediates in electro-organic chemistry. It was effective for monitoring of the generation of ArS(ArSSAr)$^+$ by the electrochemical oxidation of ArSSAr (Ar = p-FC$_6$H$_4$) in Bu$_4$NBF$_4$/CH$_2$Cl$_2$ at 195 K. The intensity of a Raman band at 427 cm^{-1}, which is attributable to the S-S vibration of ArS(ArSSAr)$^+$, increased with an increase in the electricity until 2/3 F of the electricity was consumed, whereas decreased with a further increase in the electricity indicating decomposition of ArS(ArSSAr)$^+$.

Raman spectroscopy has been a common tool for the study of complex molecular systems in organic chemistry, coordination chemistry, biochemistry, and various fields in nanosciences.[1] Recent applications include the metal-ligand interaction in organogold clusters, Au$_{54}$(C≡CPh)$_{26}$,[2] and π-π interaction in linear polyyne molecules, H(C≡C)$_n$H (n = 4-8), accommodated inside single-walled carbon nanotubes (SWNT).[3] Recent developments in laser Raman techniques lead to the detection of highly reactive and unstable intermediates.[4]

Raman scattering spectroscopy is complementary to the infrared (IR) absorption spectroscopy. On the contrary to the IR spectroscopy which mainly focuses on the detection of *polar* substituent groups in a molecule,[1a] Raman spectroscopy is advantageous in the detection of vibrational mode signals of *nonpolar* homo-nuclear bonding. Moreover, Raman spectroscopy is applicable not only to the detection of the local-mode vibration, but also to the characterization of a number of collective vibrations appearing as low-frequency Raman-mode signals for which a sequence of skeletal C-C or S-S bonds are involved. Furthermore, such vibrational-mode signals of lower frequencies at <500 cm^{-1}, which are not accessible in conventional IR spectroscopy, are readily accessible by Raman spectroscopy. Therefore, it is useful for characterization of the molecular structure as well as of the nature of the chemical bonding.[1a] To extend the applicability of Raman spectroscopy to the detection of reactive intermediates which are stable only under low temperatures, we have developed an *in situ* Raman spectroscopic measurement system for monitoring of the preparative electrochemical reaction in a liquid phase at low temperatures.

We focus on the low temperature electrochemical oxidation[5-9] of diaryl disulfides, ArSSAr,[6] to generate and accumulate arylbis(arylthio)sulfonium ions, ArS(ArSSAr)$^+$, which serve as useful intermediates for various transformation schemes.[7] The formation of the ion, ArS(ArSSAr)$^+$, was well characterized by ^{1}H NMR and cold-spray-ionization mass spectrometry (CSI-MS).[8] However, the detailed mechanism for the formation of ArS(ArSSAr)$^+$ still remains unclear. We envisaged that *in situ* vibrational Raman spectroscopy would certainly be a powerful tool for elucidating the chemical composition and the molecular structure of ArS(ArSSAr)$^+$.

In this Communication, we wish to present *in situ* Raman spectroscopic detection and monitoring of ArS(ArSSAr)$^+$, during its generation and accumulation by the electrochemical oxidation of ArSSAr at 195 K. To the best of our knowledge, this is the first report on an *in situ* Raman spectroscopic study in electro-organic chemistry involving unstable intermediates at low temperatures.

Electrochemical Oxidation

$$3\ \mathrm{ArSSAr} \xrightarrow[\mathrm{Bu_4NBF_4/CH_2Cl_2}]{-2e,\ 195\ \mathrm{K}} \left[\begin{array}{c} 2\ \mathrm{ArS^+} \\ + \\ 2\ \mathrm{ArSSAr} \end{array}\right] \longrightarrow 2\ \mathrm{ArS(ArSSAr)^+} \qquad (1)$$

(Ar = p-FC$_6$H$_4$)

in situ Raman spectroscopy

Our aim herein is to record vibrationally resolved Raman scattering signals of ArS(ArSSAr)$^+$ (eq. 1),[10-12] which is assumed to possess a skeletal S$_3$ moiety in a triangular form. According to the stoichiometry represented in eq. 1, three reactant molecules with two leaving electrons form two target ions. Thus, 2/3 F of electricity to the initial amount of ArSSAr are necessary for complete conversion into ArS(ArSSAr)$^+$. First, we set up a custom-made Raman spectroscopic measurement system using 785 nm laser excitation and a cold probe suitable for the operation at ~195 K (Fig. 1). Second, electrochemical processes generating ArS(ArSSAr)$^+$ were observed by recording a series of Raman spectra during the electrolysis. Finally, molecular orbital calculations were performed for the assignment of observed Raman scattering signals as well as for understanding of the chemical process during the electrolysis. For further experimental details, see Electronic Supplementary Information (ESI).

Prior to the electrolysis, Raman spectra were recorded at ambient temperature for the reactant molecules (neat), ArSSAr (Ar = p-FC$_6$H$_4$), as shown in Fig. 2 (thick line in blue). In the spectral region above ~1000 cm^{-1}, Raman bands are attributable to in-plane deformations in the *para*-fluorophenyl group, whereas

Raman spectral features below ~1000 cm^{-1} are attributable to out-of-plane deformations as well as the other modes including C-S and S-S vibrations. According to the calculated Raman spectrum in Fig. 2 (thin line in black),13 the observed Raman signal at 1076 cm^{-1} is assigned to a characteristic C-S stretching mode strongly coupled with deformation of the phenyl groups (ring breathing mode), which is relevant to the displacement vectors illustrated in the inset. The spectral features are comparable to those for an analogous molecule of PhSSPh (Ph = C_6H_5).[14]

When ArSSAr (Ar = *p*-FC_6H_4), was dissolved in the solvent, CH_2Cl_2, the bands of ArSSAr were discernible as superposition of the reactant spectrum to the solvent spectrum. This indicated that the solvent effect was fairly negligible, at least, for the neutral molecules of ArSSAr. When the electrolyte, Bu_4NBF_4, was added to the solution, relevant ions of Bu_4N^+ and BF_4^- were confirmed by their Raman bands in >850 cm^{-1}. At this stage, The Raman spectrum in the low frequency region of 300-650 cm^{-1} was dominated by the spectral features of ArSSAr (see Fig. S1 in ESI). We focused on the spectral change in this low-frequency region below 850 cm^{-1}, where the vibrational modes of C-S and S-S bonds are responsible.

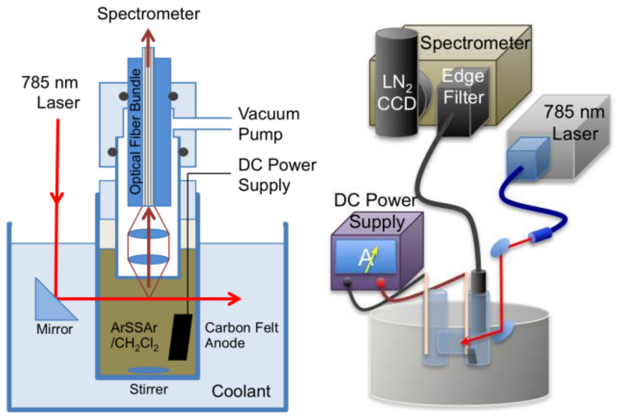

Fig. 1 Schematics for the optical probe operated at 195 K (left) for the *in situ* Raman spectroscopic measurement system (right).

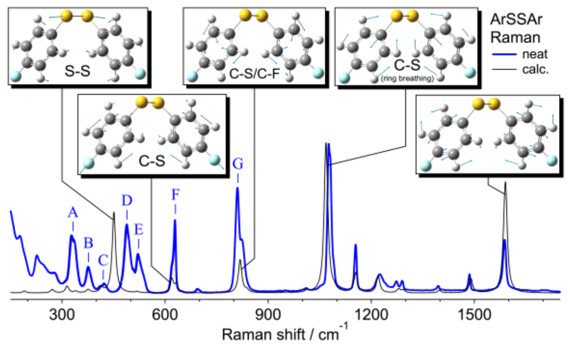

Fig. 2 Raman spectrum of ArSSAr (Ar = *p*-FC_6H_4) (neat) at ambient temperature before electrolysis (thick line in blue) compared with the calculated Raman spectrum at B3LYP/6-311++G(2d,p) level of theory[13] (thin line in black). The calculated frequency is scaled by a factor of 0.98 for possible anharmonicity. Insets show calculated displacement vectors for each of the selected normal mode vibrations.

Fig. 3 shows a series of Raman spectra with the excitation at 785 nm recorded during the electrolysis of ArSSAr at 195 K under the presence of Bu_4NBF_4 as supporting electrolyte in the solvent of CH_2Cl_2. Even at the low temperature of 195 K, the spectral features for ArSSAr were identical to those observed at ambient temperature as indicated by peaks A-G in both Fig. 2 and the bottom trace in Fig. 3. The signal intensity in Fig. 3 was much weaker because of the sample being a dilute solution. Observed also in the solution, the Raman spectral features, A-G, belong to isolated ArSSAr molecules. As time went along the electrolysis (see the series of spectra from bottom to top), the spectral features A-G diminished, e.g., at 491, 523, and 812 cm^{-1}, whereas Raman bands at 328, 427, 489, 628, and 817 cm^{-1} newly appeared.

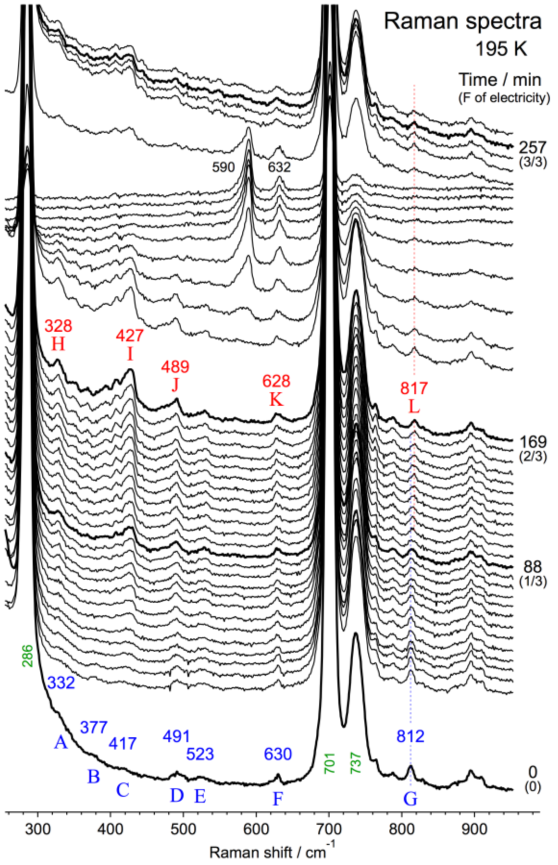

Fig. 3 Raman spectra recorded during the electrolysis at 195 K; from bottom to top, spectra accumulated for every 400 seconds (6.67 minutes) over the end of the reaction at 270 minutes. Major peaks at 286, 701, and 737 cm^{-1} belong to the solvent of CH_2Cl_2. Raman bands indicated by A-G in the bottom trace belong to the reactant, ArSSAr (Ar = *p*-FC_6H_4), and are corresponding to those noted by A-G in Fig. 2, whereas Raman bands indicated by H-L in an upper trace are attributable to the product, $ArS(ArSSAr)^+$.

To elucidate the optimum electricity, it is indicative to plot the intensity of selected Raman bands as a function of time for the electrolysis as shown in Fig. 4. The electrolysis current was kept constant at 8.0 mA throughout the experiment, thus the plot is understood as a function of the integrated current consumed. Solid circles in red represent the intensity of the Raman band I at 427 cm^{-1}. Its intensity increased proportionally to the increasing time for the electrolysis. We attributed it to a Raman signal of

$ArS(ArSSAr)^+$, which was gradually accumulated in the solution. Solid triangles in blue represent the intensity of the Raman band G at 812 cm^{-1}, the C-S/C-F stretching mode in ArSSAr (see Fig. 2). Its intensity decreased as the electrolysis proceeded. Note here that, in Fig. 3, another band L at 817 cm^{-1} was appearing with increasing intensity in the close vicinity of the decreasing band G at 812 cm^{-1}. The signal of the band G at 812 cm^{-1} for ArSSAr disappeared completely at 169 min in Fig. 3, up to which 2/3 F of electricity had been consumed.

Proportionality to the consumed current of the Raman intensity at 427 cm^{-1} (band I) confirms accumulation of $ArS(ArSSAr)^+$ in the solution at a constant rate during the electrochemical oxidation of ArSSAr. After 2/3 F of electricity was consumed, the yellow solution began to turn into brownish and the excitation laser beam became absorbed substantially at the entrance of the glass cell. At this point, another signal of light scattering appeared at a Raman shift of 590 cm^{-1} accompanied by a satellite band at 632 cm^{-1} (see Fig. 3). These additional features remained up to the point at 3/3 F of electricity to the initial amount of ArSSAr. Afterwards, transparency of the solution resumed and the signal of the sulfonium ion became observable again at 427 cm^{-1} (band I). These observations indicate that additional oxidation in the system might cause the formation of a by-product.[15] Some adducts may be relevant, possibly associated with interaction between the sulfonium ion and a solvent molecule which are the most abundant species in the system.

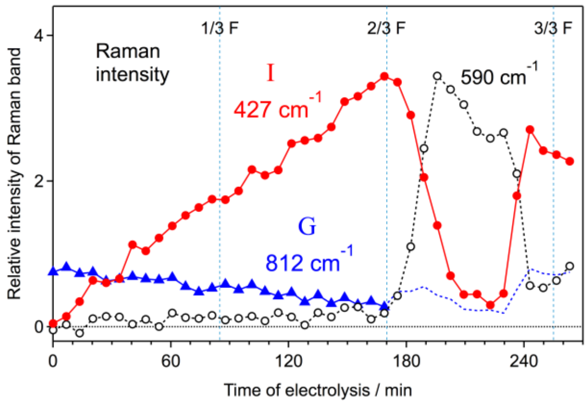

Fig. 4 Intensity profiles of selected Raman bands as a function of time of electrolysis. Current for the electrolysis was fixed at 8.0 mA throughout the experiment. Plots correspond to the band I for sulfonium ion, $ArS(ArSSAr)^+$, (●), the band G for disulfide, ArSSAr, (▲), and the band at 590 cm^{-1} for a by-product (○).

Concerning the reaction mechanism, the present experimental result is consistent with a proposed model,[7f] in which 2/3 F of electricity is consumed for the stoichiometric conversion of disulfide, ArSSAr, to the trimer cation, $ArS(ArSSAr)^+$ (see eq. 1). The electrolysis should be turned off for avoiding unnecessary side reactions, provided that the suitable current of 2/3 F of electricity is applied. The low-temperature *in situ* monitoring of the Raman scattering intensity for the target ion, $ArS(ArSSAr)^+$, is of great help in preparation of a “cation pool”.[16]

Fig. 5 compares the experimental spectrum at 169 min (2/3 F) in Fig. 3 (thick line in red) with the calculated Raman spectrum for the trimeric sulfonium ion, $ArS(ArSSAr)^+$, (thin line in black). Insets show the optimized geometry for $ArS(ArSSAr)^+$ with displacement vectors for the relevant vibrational mode. Three sulphur atoms locate in a bent form with the S-S-S angle of 104° and S-S bond lengths of ~2.17Å, slightly elongated from 2.11Å for the S-S bond in ArSSAr.

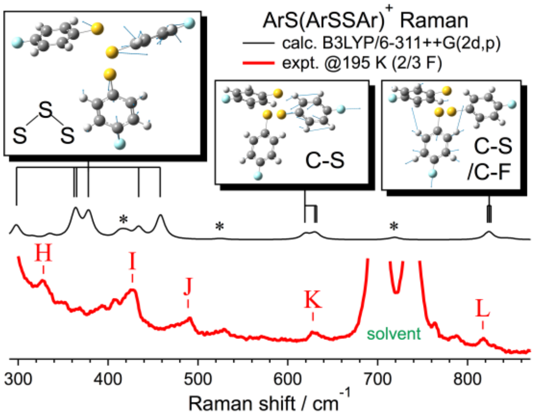

Fig. 5 The experimental spectrum (thick line in red) at 2/3 F of electricity showing bands H-L for $ArS(ArSSAr)^+$ (Ar = *p*-FC_6H_4) compared with the calculated Raman spectrum at B3LYP/6-311++G(2d,p) (thin line in black).[13] Displacement vectors are illustrated for three normal modes of S-S, C-S, and C-S/C-F vibrations. Asterisks indicate weak Raman modes of out-of-plane ring deformations. Calculated vibrational frequency is scaled by a factor of 0.98.

For high-frequency modes in >500 cm^{-1}, whose motions are localized in a monomer unit of ArS (Ar = *p*-FC_6H_4), only a small frequency shift is expected, since a band of three-fold vibrational modes of the same type in the trimer, $ArS(ArSSAr)^+$, appears in the close vicinity of the band of two-fold modes of the same type in the dimer, ArSSAr, as observed in the intensity alternations from the band F (630 cm^{-1}) to K (628 cm^{-1}) and from G (812 cm^{-1}) to L (817 cm^{-1}) in Fig. 3. New vibrational degrees of freedom created upon the trimer formation are six intermolecular vibrations. Most of them are low-frequency modes in <100 cm^{-1}, whereas, in case where an intermolecular S-S bond is newly formed, one of the six frequencies comes in 300-500 cm^{-1} and the S-S motions can be coupled to another existing S-S motions as well as to the other motions of similar frequencies to enhance some lower frequency Raman signals.

The newly observed bands in-between H and J including the prominent band I at 427 cm^{-1} in Fig. 5 are explainable by two modes in a bent S_3 moiety, symmetric stretch and anti-symmetric stretch, and several S_3 modes coupled with out-of-plane and in-plane deformations of the phenyl rings. Sticks in 295-470 cm^{-1} in Fig. 5 indicate the calculated S_3-oriented vibrational Raman modes, whereas asterisks depict weaker Raman bands of some uncoupled ring deformation modes. For the assignment in more detail, see also ESI.

Conclusions

We demonstrated *in situ* Raman spectroscopic studies of intermediate species generated under the electrochemical oxidation of ArSSAr into $ArS(ArSSAr)^+$ at 195 K. The Raman signal at 427 cm^{-1} appeared as the anodic oxidation proceeds, which we attributed to the trimer cation, $\mathrm{ArS(ArSSAr)^+}$. Stoichiometry was confirmed from time profiles for the Raman scattering intensity of individual chemical species. The low-temperature Raman spectroscopic probe developed in this work was successfully applied to monitoring of unstable intermediates generated in the electrochemical reaction at low temperature. Further applications of this optical-probe system to synthetic chemistry are currently under investigation in our laboratory.

Acknowledgments

This work was supported in part by Grant-in-Aid from the Ministry of Education, Culture, Sports, Science and Technology (MEXT), No. 26410059, and by MEXT-Supported Program for the Strategic Research Foundation at Private Universities, subsidy from MEXT and Kindai University. K. M. thanks Sasakawa Scientific Research Grant from The Japan Science Society for financial support. T. W. and Y. M. were supported by the Research Budget No. 26 in 2014 from Graduate School of Science and Engineering, Kindai University.

Notes and references

[a] *Department of Chemistry, School of Science and Engineering, Kindai University, Kowakae 3-4-1, Higashi-Osaka, Osaka 577-8502, Japan; Fax: +81-6-6723-2721; Tel: +81-6-4307-3408; E-mail: kmatsumo@chem.kindai.ac.jp, wakaba@chem.kindai.ac.jp*

[b] *Department of Chemistry, LMU München, Butenandtstrasse 5-13, D-81377 München, Germany Fax: +49-89-218077738; Tel: +49-89-218077737; E-mail: zipse@cup.uni-muenchen.de*

[c] *Graduate School of Natural Science and Technology, Okayama University, Tsuhsima-Naka 3-1-1, Kita-ku, Okayama 700-8530, Japan; Fax: +81-86-251-8081; Tel: +81-86-251-8081; E-mail: suga@cc.okayama-u.ac.jp*

[d] *Department of Synthetic Chemistry and Biological Chemistry, Graduate School of Engineering, Kyoto University, Nishikyo-ku, Kyoto 615-8510, Japan; Fax: +81-75-383-2727; Tel: +81-75-383-2726; E-mail: yoshida@sbchem.kyoto-u.ac.jp*

† Electronic Supplementary Information (ESI) available: [details of any supplementary information available should be included here]. See DOI: 10.1039/b000000x/

1 (a) K. Nakamoto, *Infrared and Raman Spectra of Inorganic and Coordination Compounds*, *Part A and Part B*, 6th Edn., Wiley-Interscience, 2008; (b) V. Stancovski and S. Badilescu, *J. Appl. Electrochem.*, 2014, **44**, 23; (c) M. S. Dresselhaus, A. Jorio and R. Saito, *Annu. Rev. Condens. Matter Phys.*, 2010, **1**, 89.

2 (a) P. Maity, T. Wakabayashi, N. Ichikuni, H. Tsunoyama, S. Xie, M. Yamauchi and T. Tsukuda, *J. Chem. Soc., Chem. Commun.*, 2012, **48**, 6085; (b) P. Maity, S. Takano, S. Yamazoe, T. Wakabayashi and T. Tsukuda, *J. Am. Chem. Soc.*, 2013, **135**, 9450.

3 (a) D. Nishide, H. Dohi, T. Wakabayashi, E. Nishibori, S. Aoyagi, M. Ishida, S. Kikuchi, R. Kitaura, T. Sugai, M. Sakata and H. Shinohara, *Chem. Phys. Lett.*, 2006, **428**, 356; (b) D. Nishide, T. Wakabayashi, T. Sugai, R. Kitaura, H. Kataura, Y. Achiba and H. Shinohara, *J. Phys. Chem. C*, 2007, **111**, 5178; (c) T. Wakabayashi, T. Murakami, H. Nagayama, D. Nishide, H. Kataura, Y. Achiba, H. Tabata, S. Hayashi and H. Shinohara, *Eur. Phys. J. D*, 2009, **52**, 79.

4 The *in situ* Raman spectroscopic detection of electrochemically generated unstable intermediate has reported. See, T. Marui, S. Kajita, Y. Katayama and K. Chiba, *Electrochem. Commun.*, 2007, **9**, 1331.

5 For electro-organic chemistry, (a) K. D. Moeller, *Tetrahedron*, 2000, **56**, 9527; (b) J. M. Savéant, *Chem. Rev.*, 2008, **108**, 2348; (c) K. A. Ogawa and A. J. Boydston, *Chem. Lett.*, 2015, **44**, 10; (d) R. Francke and R. D. Little, *Chem. Soc. Rev.*, 2014, **43**, 2492; (e) F. Tang, C. Chen and K. D. Moeller, *Synthesis*, 2007, **21**, 3411; (f) J. Yoshida, K. Kataoka, R. Horcajada and A. Nagaki, *Chem. Rev.*, 2008, **108**, 2265; (g) J. B. Sperry and D. L. Wright, *Chem. Soc. Rev.*, 2006, **35**, 605; (h) H. Lund, *J. Electrochem. Soc.*, 2002, **149**, S21; (i) *Organic Electrochemistry*, ed. H. Lund and O. Hammerich, Dekker, New York, 2nd Edn., 2001.

6 (a) A. Bewick, D. E. Coe, J. M. Mellor and D. J. Walton, *J. Chem. Soc., Chem. Commun.*, 1980, 51; (b) S. Boryczka, D. Elothmani, Q. T. Do, J. Simonet and G. L. Guillanton, *J. Electrochem. Soc.*, 1996, **143**, 4027; (c) S. Töteberg-Kaulen and E. Steckhan, *Tetrahedron*, 1988, **44**, 4389; (d) Q. T. Do, D. Elothmani, J. Simonet and G. L. Guillanton, *Electrochim. Acta*, 2005, **50**, 4792, and references therein.

7 (a) S. Suga, K. Matsumoto, K. Ueoka and J. Yoshida, *J. Am. Chem. Soc.*, 2006, **128**, 7710; (b) K. Matsumoto, S. Fujie, K. Ueoka, S. Suga and J. Yoshida, *Angew. Chem., Int. Ed.*, 2008, **47**, 2506; (c) K. Matsumoto, K. Ueoka, S. Fujie, S. Suga and J. Yoshida, *Heterocycles*, 2008, **76**, 1103; (d) K. Matsumoto, S. Fujie, S. Suga, T. Nokami and J. Yoshida, *Chem. Commun.*, 2009, 5448; (e) S. Fujie, K. Matsumoto, S. Suga and J. Yoshida, *Chem. Lett.*, 2009, **38**, 1186; (f) K. Matsumoto, K. Ueoka, S. Suzuki, S. Suga and J. Yoshida, *Tetrahedron*, 2009, **65**, 10901; (g) S. Fujie, K. Matsumoto, S. Suga, T. Nokami and J. Yoshida, *Tetrahedron*, 2010, **66**, 2823; (h) K. Saito, K. Ueoka, K. Matsumoto, S. Suga, T. Nokami and J. Yoshida, *Angew. Chem., Int. Ed.*, 2011, **50**, 5153; (i) K. Saito, Y. Saigusa, T. Nokami and J. Yoshida, *Chem. Lett.*, 2011, **40**, 678; (j) K. Matsumoto, Y. Kozuki, Y. Ashikari, S. Suga, S. Kashimura and J. Yoshida, *Tetrahedron Lett.*, 2012, **53**, 1916; (k) K. Matsumoto, T. Sanada, H. Shimazaki, K. Shimada, S. Hagiwara, S. Fujie, Y. Ashikari, S. Suga, S. Kashimura and J. Yoshida, *Asian J. Org. Chem.*, 2013, **2**, 325.

8 K. Yamaguchi, *J. Mass Spectrom.*, 2003, **38**, 473.

9 (a) J. Yoshida, Y. Ashikari, K. Matsumoto and T. Nokami, *J. Synth. Org. Chem., Jpn.*, 2013, **71**, 1136; (b) K. Matsumoto, S. Suga and J. Yoshida, *Org. Biomol. Chem.*, 2011, **9**, 2586.

10 (a) A. S. Gybin, W. A. Smit, V. S. Bogdanov, M. Z. Krimer and J. B. Kalyan, *Tetrahedron Lett.*, 1980, **21**, 383; (b) V. S. Bogdanov, A. S. Gybin, E. G. Cherepanova and W. A. Smith, *Izv. Akad. Nauk Ser. Khim.*, 1981, 2681.

11 K. Lam and W. E. Geiger, *J. Org. Chem.*, 2013, **78**, 8020.

12 Monomeric cation, $\mathrm{ArS^+}$, is considered to be unstable. See for example, T. Brinck, P. Carlqvist, A. H. Holm and K. Daasbjerg, *J. Phys. Chem. A*, 2002, **106**, 8827.

13 Gaussian 09, Revision C.01, M. J. Frisch, G. W. Trucks, H. B. Schlegel, G. E. Scuseria, M. A. Robb, J. R. Cheeseman, G. Scalmani, V. Barone, B. Mennucci, G. A. Petersson, H. Nakatsuji, M. Caricato, X. Li, H. P. Hratchian, A. F. Izmaylov, J. Bloino, G. Zheng, J. L. Sonnenberg, M. Hada, M. Ehara, K. Toyota, R. Fukuda, J. Hasegawa, M. Ishida, T. Nakajima, Y. Honda, O. Kitao, H. Nakai, T. Vreven, J. A. Montgomery, Jr., J. E. Peralta, F. Ogliaro, M. Bearpark, J. J. Heyd, E. Brothers, K. N. Kudin, V. N. Staroverov, T. Keith, R. Kobayashi, J. Normand, K. Raghavachari, A. Rendell, J. C. Burant, S. S. Iyengar, J. Tomasi, M. Cossi, N. Rega, J. M. Millam, M. Klene, J. E. Knox, J. B. Cross, V. Bakken, C. Adamo, J. Jaramillo, R. Gomperts, R. E. Stratmann, O. Yazyev, A. J. Austin, R. Cammi, C. Pomelli, J. W. Ochterski, R. L. Martin, K. Morokuma, V. G. Zakrzewski, G. A. Voth, P. Salvador, J. J. Dannenberg, S. Dapprich, A. D. Daniels, O. Farkas, J. B. Foresman, J. V. Ortiz, J. Cioslowski and D. J. Fox, Gaussian, Inc., Wallingford CT, 2010.

14 L. M. S. Takata, A. C. Gonçalves, R. A. Ando, A. A. D. Santos and P. H. C. Camargo, *J. Raman. Spectrosc.*, 2012, **43**, 712.

15 (a) K. Yamamoto, E. Tsuchida, H. Nishide, S. Yoshida and Y. S. Park, *J. Electrochem. Soc.*, 1992, **139**, 2401, (b) F. Aida, Y. Takatori, D. Kiyokawa, K. Nagamatsu, H. Nishide and Y. Oyaizu, *Chem. Lett.*, 2015, **44**, 767, and references therein.

16 For recent reports on the "cation pool" method, (a) Y. Ashikari, Y. Kiuchi, T. Takeuchi, K. Ueoka, S. Suga and J. Yoshida, *Chem. Lett.*, 2014, **43**, 210; (b) Y. Ashikari, A. Shimizu, T. Nokami and J. Yoshida, *J. Am. Chem. Soc.*, 2013, **135**, 16070; (c) T. Nokami, T. Watanabe, K. Terao, K. Soga, K. Ohata and J. Yoshida, *Electrochemistry*, 2013, **81**, 399; (d) Y. Ashikari, T. Nokami and J. Yoshida, *Org. Biomol. Chem.*, 2013, **11**, 3322.